Acta Cryst E CRYSTALLOGRAPHIC COMMUNICATIONS

ISSN 2056-9890

Crystal structure of poly[(μ_3-4-amino-1,2,5-oxadiazole-3-hydroxamato)thallium(I)]

Inna S. Safyanova,[a]* Oksana A. Bondar,[a] Anna V. Pavlishchuk,[a] Iryna V. Omelchenko,[b] Turganbay S. Iskenderov[a] and Valentina A. Kalibabchuk[c]

[a]Department of Chemistry, National Taras Shevchenko University of Kyiv, Volodymyrska Street 64, Kyiv, 01601, Ukraine, [b]SSI "Institute for Single Crystals", National Academy of Sciences of Ukraine, Nauky ave. 60, 61001 Kharkiv, Ukraine, and [c]Department of General Chemistry, O.O. Bohomolets National Medical University, Shevchenko Blvd. 13, 01601 Kyiv, Ukraine. *Correspondence e-mail: sssafyanova@gmail.com

Received 18 November 2019
Accepted 4 February 2020

Edited by M. Weil, Vienna University of Technology, Austria

Keywords: crystal structure; 1,2,5-oxadiazole; hydroxamic acid; thallium(I); tautomerism.

CCDC reference: 1981874

Supporting information: this article has supporting information at journals.iucr.org/e

The title compound represents the thallium(I) salt of a substituted 1,2,5-oxadiazole, $[Tl(C_3H_3N_4O_3)]_n$, with amino- and hydroxamate groups in the 4- and 3- positions of the oxadiazole ring, respectively. In the crystal, the deprotonated hydroxamate group represents an intermediate between the keto/enol tautomers and forms a five-membered chelate ring with the thallium(I) cation. The coordination sphere of the cation is augmented to a distorted disphenoid by two monodentately binding O atoms from two adjacent anions, leading to the formation of zigzag chains extending parallel to the *b* axis. The cohesion within the chains is supported by π–π stacking [centroid–centroid distance = 3.746 (3) Å] and intermolecular N—H···N hydrogen bonds.

1. Chemical context

Substituted oxadiazoles attract attention because of their wide range of applications in organic synthesis as useful intermediates (Romeo & Chiacchio, 2011; Zlotin *et al.*, 2017) and for drug design (Giorgis *et al.*, 2011; Pal *et al.*, 2017; Stepanov *et al.*, 2015). In addition, molecules with the oxadiazole moiety can be considered for the creation of energetic systems (Zhang *et al.*, 2015) with high thermal stability and mechanical sensitivity. The variety of coordination modes typical for oxadiazole-containing ligands result in the formation of multiple mono- and polynuclear complexes, as well as coordination polymers (Akhbari & Morsali, 2010). Complexes with oxadiazole-based ligands have demonstrated significant biological activity as anti-cancer (Glomb *et al.*, 2018), anti-inflammatory (Singh *et al.*, 2013), anti-tuberculosis (De *et al.*, 2019) and anti-malarial (Zareef *et al.*, 2007) agents.

However, the standard synthetic procedures for oxadiazole-containing scaffolds usually utilizes the dehydrative cyclization of bis-oximes, which is performed at high temperatures (Fershtat & Makhova, 2016; Romeo & Chiacchio, 2011) and often includes the introduction of different activating reagents (Shaposhnikov *et al.*, 2003; Telvekar & Takale, 2013). A convenient procedure for the synthesis of substituted 4-amino-1,2,5-oxadiazoles based on the formation of bis-oximes *in situ* from the hydroxylamine and cyano-oximes was recently proposed (Neel & Zhao, 2018). The introduction of dehydrating agents allows a significant decrease in the temperature during reaction, gave the possibility to synthesize substituted 1,2,5-oxadiazoles with various side functional groups. In this regard, we have adapted the synthetic procedure for 1,2,5-oxadiazole with amino- and hydroxamate groups in the 4- and

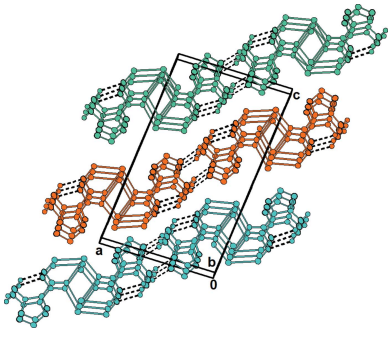

3- position of the 1,2,5-oxadiazole ring, respectively, and report here the thallium(I) salt of this compound, **1**, $Tl(C_3H_3N_4O_3)$. The introduction of a hydroxamic group at the 1,2,5-oxadiazole ring allows the consideration of potentially interesting ligand systems for the synthesis of various polynuclear complexes (Pavlishchuk *et al.*, 2018; Lutter *et al.*, 2018; Ostrowska *et al.*, 2019; Gumienna-Kontecka *et al.*, 2007).

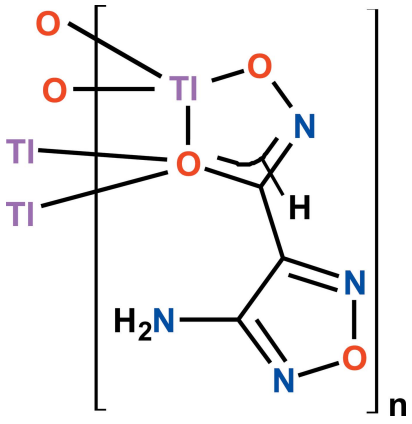

2. Structural commentary

The asymmetric unit of **1** comprises one 4-amino-1,2,5-oxadiazole-3 hydroxamate anion and a thallium(I) cation. The oxadiazole ring C2/C3/N2/O3/N3 is almost planar with the largest deviation from the least-squares plane being 0.007 Å for C2. The C2═N2 and C3═N3 bond lengths [1.304 (14) and 1.329 (11) Å, respectively] are typical for C═N double bonds in substituted oxadiazole cycles (Viterbo & Serafino, 1978), and the N2—O3 and N3—O3 bonds [1.365 (11) and 1.419 (11) Å, respectively] also fall in a range typical for 1,2,5-oxadiazoles (Fonari *et al.*, 2003; Viterbo & Serafino, 1978). The substituent amino- and hydroxamate groups in the 4- and 3- positions, respectively, of the 1,2,5-oxadiazole ring are nearly coplanar with the oxadiazole ring, with a deviation of 0.071 Å for nitrogen atom N4 of the amino group and a dihedral angle between the mean plane of the heterocycle and the hydroxamate group C1/O2/N1/O1 of 8.4 (4)°. The C3—N4 [1.360 (13) Å] and N1—O1 [1.412 (9) Å] bond lengths are typical for a non-coordinating amino group (Fonari *et al.*, 2003; Viterbo & Serafino, 1978) and for a deprotonated hydroxamate group (Golenya *et al.*, 2012; Safyanova *et al.*, 2017), respectively. On the other hand, the C1—N1 [1.314 (12) Å] and C1—O2 [1.275 (11) Å] bond lengths are intermediate between the tautomeric keto and enol forms (Larsen, 1988), accompanied by a delocalization of the π electrons over the N1—C1—O2 backbone and a disorder of the corresponding hydrogen atom that could not be localized from difference-Fourier maps.

The Tl1 cation in **1** is bonded to the bidentate hydroxamate anion through oxygen atoms O1 [2.814 (7) Å] and O2 [2.537 (7) Å] in the form of a five-membered chelate ring. The coordination sphere of the Tl1 cation in **1** is augmented to four by two monodentately binding O2 atoms of two adjacent oxadiazole moieties with distances of Tl1—$O2^{ii}$ = 2.880 (7) Å and Tl1—$O2^{i}$ = 2.761 (7) Å [symmetry codes: (i) $-x, y+\frac{1}{2}, -z+\frac{3}{2}$; (ii) $-x, y-\frac{1}{2}, -z+\frac{3}{2}$] (Fig. 1). The bond length Tl1—O2 is *ca* 0.2–0.3 Å shorter in the case of the chelating coordination mode of the hydroxamate group compared with the monodentate coordination mode. Thus, each O2 atom is involved in a chelate coordination with one Tl1 ion and in a monodentate coordination with two other Tl1 ions, forming zigzag chains extending along the *b*-axis direction (Fig. 2). The Tl—O bond lengths involving the hydroxamate oxygen atoms in **1** are typical for Tl^{I} compounds (Salassa & Terenzi, 2019), and the formation of similar polymeric chains is frequently observed for Tl^{I} complexes (Akhbari *et al.*, 2009). The resulting coordination sphere of Tl1 can be best described as a distorted seesaw (SS-4) or disphenoid with a stereochemically active lone pair (Mudring & Rieger, 2005). If longer bonds are taken into account (Akhbari & Morsali, 2010; Schroffenegger *et al.*, 2020), the Tl1 cation also has weak interactions at 3.453 (8), 3.289 (9), 3.385 (7) and 3.219 (8) Å with $O3^{iv}$, $N2^{ii}$, $O1^{v}$ and $O3^{vi}$ [symmetry codes: (iv) $x, -y+\frac{3}{2}, z+\frac{1}{2}$; (v) $x, y+1, z$; (vi) $x,$

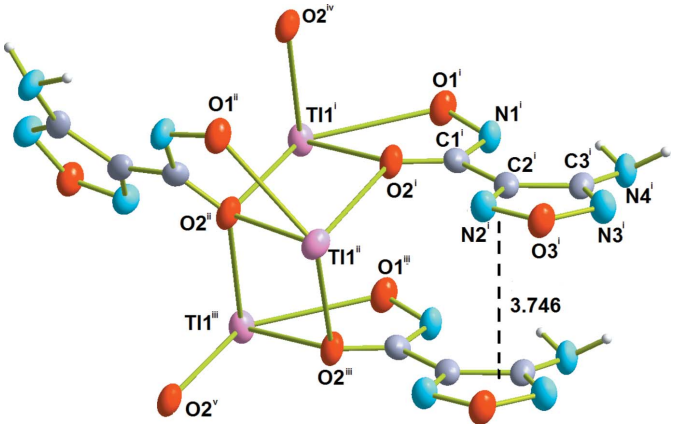

Figure 1
A fragment of the crystal structure of **1** showing the coordination environment of the Tl1 ions with displacement ellipsoids drawn at the 50% probability level. [Symmetry codes: (i) $1+x, y, z$; (ii) $1-x, \frac{1}{2}+y, \frac{3}{2}-z$; (iii) $1+x, 1+y, z$; (iv) $1-x, -\frac{1}{2}+y, \frac{3}{2}-z$; (v) $1-x, \frac{3}{2}+y, \frac{3}{2}-z$.]

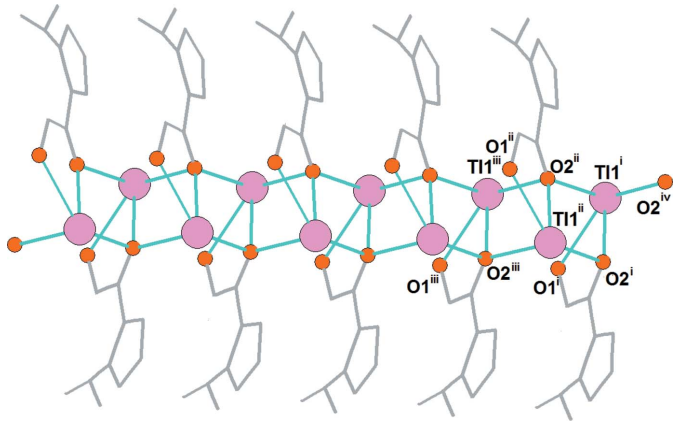

Figure 2
The formation of polymeric zigzag chains in **1.** [Symmetry codes: (i) $1+x, y, z$; (ii) $1-x, \frac{1}{2}+y, \frac{3}{2}-z$; (iii) $1+x, 1+y, z$; (iv) $1-x, -\frac{1}{2}+y, \frac{3}{2}-z$; (v) $1-x, \frac{3}{2}+y, \frac{3}{2}-z$.]

Table 1
Hydrogen-bond geometry (Å, °).

D—H···A	D—H	H···A	D···A	D—H···A
N4—H4A···N3^{i}	0.93	2.23	3.156 (10)	169
N4—H4B···N1^{ii}	1.01	2.65	3.256 (13)	118

Symmetry codes: (i) $-x+1, -y, -z+1$; (ii) $-x+1, y-\frac{1}{2}, -z+\frac{3}{2}$.

$-y+\frac{1}{2}, z+\frac{1}{2}$] atoms from another three oxadiazole moieties. The closest contact between adjacent Tl1 cations within a zigzag chain is 3.7458 (5) Å.

3. Supramolecular features

In the crystal, the oxadiazole rings are stacked in a parallel manner with a centroid–centroid distance = 3.746 (3) Å (Fig. 1). Together with weak intermolecular hydrogen bonds between the amino group (N4) and two nitrogen atoms from the azolo (N3) and the hydroxamic (N1) group (Table 1, Fig. 3) they support the cohesion of the chains along the *b*-axis direction.

4. Database survey

A search in the Cambridge Structural Database (CSD version 5.39, update of May 2018; Groom *et al.*, 2016) for substituted oxadiazoles revealed two structures, *viz.* 3-amino-4-methylfurazan (Pibiri *et al.*, 2018) and 4-amino-1,2,5-oxadiazole-3-carboxamide oxime (Zhang & Jian, 2009). Tl^{I} complexes with comparable organic ligands have been reported for thallium (anthranoyl)anthranilate (Wiesbrock & Schmidbaur, 2004), thallium(I) 2-amino-benzoate (Wiesbrock & Schmidbaur, 2003), thallium(I) arylcyanoxime (Robertson *et al.*, 2004) [$Tl_4(H_2O)_2$(anthracene-9-carboxylate)$_4$] (Kumar *et al.*, 2015), bis[(μ-1,3-diphenylpropane-1,3-dionato-*O*,*O*′:*O*′)dimethylthallium] (Britton, 2001) and thallium(I) 4-hydroxybenzylidene-4-aminobenzoate (Akhbari *et al.*, 2009).

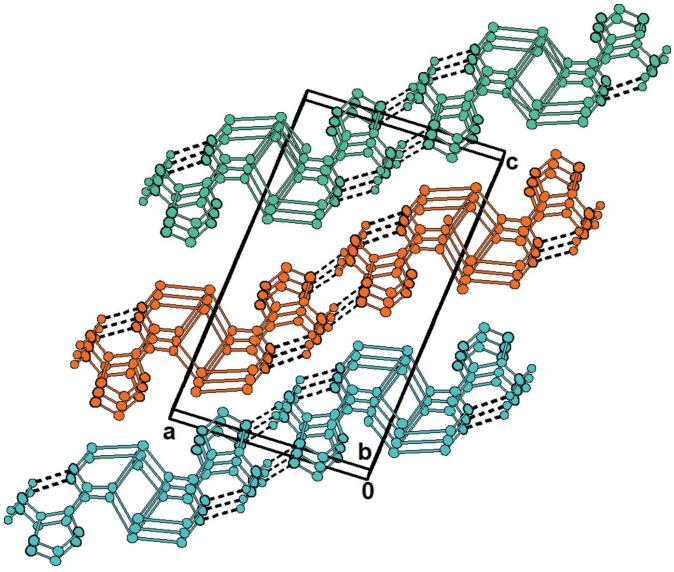

Figure 3
Packing diagram of **1**, with hydrogen bonds indicated by dashed lines.

Table 2
Experimental details.

Crystal data	
Chemical formula	[Tl($C_3H_3N_4O_3$)]
M_r	347.46
Crystal system, space group	Monoclinic, $P2_1/c$
Temperature (K)	298
a, b, c (Å)	10.0731 (4), 3.74576 (18), 16.9805 (6)
β (°)	95.808 (4)
V (Å^3)	637.41 (5)
Z	4
Radiation type	Mo $K\alpha$
μ (mm^{-1})	25.30
Crystal size (mm)	0.2 × 0.2 × 0.2
Data collection	
Diffractometer	Agilent Xcalibur Sapphire3 CCD
Absorption correction	Multi-scan (*CrysAlis PRO*; Agilent, 2012)
T_{min}, T_{max}	0.231, 1.000
No. of measured, independent and observed [$I > 2\sigma(I)$] reflections	4634, 1452, 1320
R_{int}	0.056
(sin $\theta/\lambda)_{max}$ (Å^{-1})	0.650
Refinement	
$R[F^2 > 2\sigma(F^2)]$, $wR(F^2)$, S	0.045, 0.111, 1.07
No. of reflections	1452
No. of parameters	100
H-atom treatment	H-atom parameters constrained
$\Delta\rho_{max}$, $\Delta\rho_{min}$ (e Å^{-3})	6.17, −2.23

Computer programs: *CrysAlis PRO* (Agilent, 2012), *SHELXT* (Sheldrick, 2015), *olex2.refine* (Bourhis *et al.*, 2015) and *OLEX2* (Dolomanov *et al.*, 2009).

5. Synthesis and crystallization

The title compound was obtained according to a modification of the procedure reported by Neel & Zhao (2018) (Fig. 4). Solutions containing 5 mmol of hydroxylamine hydrochloride in 10 ml of methanol, and 10 mmol of sodium methoxide in 15 ml of methanol were stirred for 30 min while cooling in an ice bath. The formed precipitate of sodium chloride was filtered off. The methanolic solutions of ethyl-2-cyano-2-(hydroxyimino)acetate (5 mmol) and hydroxylamine were combined and stirred for 5 h at room temperature. The resulting white precipitate was filtered off and dissolved in 5 ml of water, followed by HCl addition to pH = 5. The organic compound was extracted with ethyl acetate; the extract was subsequently dried over anhydrous Na_2SO_4, and the solvent was finally removed by rotary evaporation. Colorless crystals

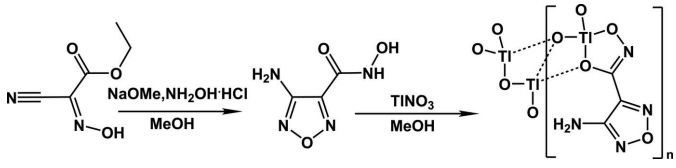

Figure 4
Synthesis scheme for 4-amino-1,2,5-oxadiazole-3 hydroxamate thallium(I).

of **1** suitable for single crystal X-ray analysis were obtained by combining the organic compound with thallium(I) nitrate in isopropanol and subsequent slow evaporation of the solvent at ambient temperature within 48 h (yield 16.5%).

6. Refinement

Crystal data, data collection and structure refinement details are summarized in Table 2. The H atoms of the amino group were located from a difference-Fourier map; their coordinates were refined freely with $U_{iso}(H) = 1.2U_{eq}(N)$. The hydrogen atom of the hydroxamate function could not be observed in difference-Fourier maps, and a tentative calculated position was in too close vicinity to atom H4*B* of the amino group. Most probably, the hydroxamate H atom is disordered over the N1—C1—O2 backbone due to the presence of both tautomeric forms. Hence, this H atom is not included in the final model. The highest remaining electron density is located 0.88 Å from Tl1.

References

Agilent (2012). *CrysAlis PRO*. Agilent Technologies Ltd, Yarnton, England.

Akhbari, K., Alizadeh, K., Morsali, A. & Zeller, M. (2009). *Inorg. Chim. Acta*, **362**, 2589–2594.

Akhbari, K. & Morsali, A. (2010). *Coord. Chem. Rev.* **254**, 1977–2006.

Bourhis, L. J., Dolomanov, O. V., Gildea, R. J., Howard, J. A. K. & Puschmann, H. (2015). *Acta Cryst.* A**71**, 59–75.

Britton, D. (2001). *Acta Cryst.* E**57**, m176–m178.

De, S., Khambete, M. P. & Degani, M. S. (2019). *Bioorg. Med. Chem. Lett.* **29**, 1999–2007.

Dolomanov, O. V., Bourhis, L. J., Gildea, R. J., Howard, J. A. K. & Puschmann, H. (2009). *J. Appl. Cryst.* **42**, 339–341.

Fershtat, L. L. & Makhova, N. N. (2016). *Russ. Chem. Rev.* **85**, 1097–1145.

Fonari, M. S., Simonov, Yu. A., Kravtsov, V. Ch., Lipkowski, J., Ganin, E. V. & Yavolovskii, A. A. (2003). *J. Mol. Struct.* **647**, 129–140.

Giorgis, M., Lolli, M. L., Rolando, B., Rao, A., Tosco, P., Chaurasia, S., Marabello, D., Fruttero, R. & Gasco, A. (2011). *Eur. J. Med. Chem.* **46**, 383–392.

Glomb, T., Szymankiewicz, K. & Świątek, P. (2018). *Molecules*, **23**, 3361–3377.

Golenya, I. A., Gumienna-Kontecka, E., Boyko, A. N., Haukka, M. & Fritsky, I. O. (2012). *Inorg. Chem.* **51**, 6221–6227.

Groom, C. R., Bruno, I. J., Lightfoot, M. P. & Ward, S. C. (2016). *Acta Cryst.* B**72**, 171–179.

Gumienna-Kontecka, E., Golenya, I. A., Dudarenko, N. M., Dobosz, A., Haukka, M., Fritsky, I. O. & Swiatek-Kozlowska, J. (2007). *New J. Chem.* **31**, 1798–1805.

Kumar, S., Sharma, R. P., Saini, A., Venugopalan, P. & Starynowicz, P. (2015). *J. Mol. Struct.* **1079**, 291–297.

Larsen, I. K. (1988). *Acta Cryst.* B**44**, 527–533.

Lutter, J. C., Zaleski, C. M. & Pecoraro, V. L. (2018). *Adv. Inorg. Chem.* 177–246.

Mudring, A. V. & Rieger, F. (2005). *Inorg. Chem.* **44**, 6240–6243.

Neel, A. J. & Zhao, R. (2018). *Org. Lett.* **20**, 2024–2027.

Ostrowska, M., Golenya, I. A., Haukka, M., Fritsky, I. O. & Gumienna-Kontecka, E. (2019). *New J. Chem.* **43**, 10237–10249.

Pal, P., Gandhi, H. P., Kanhed, A. M., Patel, N. R., Mankadia, N. N., Baldha, S. N., Barmade, M. A., Murumkar, P. R. & Yadav, M. R. (2017). *Eur. J. Med. Chem.* **130**, 107–123.

Pavlishchuk, A. V., Kolotilov, S. V., Zeller, M., Lofland, S. E. & Addison, A. W. (2018). *Eur. J. Inorg. Chem.* pp. 3504–3511.

Pibiri, I., Lentini, L., Melfi, R., Tutone, M., Baldassano, S., Galluzzo, P. R., Di Leonardo, A. & Pace, A. (2018). *Eur. J. Med. Chem.* **159**, 126–142.

Robertson, D., Barnes, C. & Gerasimchuk, N. (2004). *J. Coord. Chem.* **57**, 1205–1216.

Romeo, G. & Chiacchio, U. (2011). *Modern Heterocyclic Chemistry*, edited by J. Alvarez-Builla, J. J. Vaquero & J. Barluenga, pp. 1047–1252. Weinheim: Wiley-VCH.

Safyanova, I. S., Ohui, K. A. & Omelchenko, I. V. (2017). *Acta Cryst.* E**73**, 24–27.

Salassa, G. & Terenzi, A. (2019). *Int. J. Mol. Sci.* **20**, 3483–3500.

Schroffenegger, M., Eder, F., Weil, M., Stöger, B., Schwendtner, K. & Kolitsch, U. (2020). *J. Alloys Compd.* **820**, 153369.

Shaposhnikov, S., Pirogov, S. V., Mel'nikova, S. F., Tselinsky, I. V., Näther, C., Graening, T., Traulsen, T. & Friedrichsen, W. (2003). *Tetrahedron*, **59**, 1059–1066.

Sheldrick, G. M. (2015). *Acta Cryst.* A**71**, 3–8.

Singh, A. K., Lohani, M. & Parthsarthy, R. (2013). *Iran. J. Pharm. Res.* **12**, 319–323.

Stepanov, A. I., Astrat'ev, A. A., Sheremetev, A. B., Lagutina, N. K., Palysaeva, N. V., Tyurin, A. Yu., Aleksandrova, N. S., Sadchikova, N. P., Suponitsky, K. Yu., Atamanenko, O. P., Konyushkin, L. D., Semenov, R. V., Firgang, S. I., Kiselyov, A. S., Semenova, M. N. & Semenov, V. V. (2015). *Eur. J. Med. Chem.* **94**, 237–251.

Telvekar, V. N. & Takale, B. S. (2013). *Synth. Commun.* **43**, 221–227.

Viterbo, D. & Serafino, A. (1978). *Acta Cryst.* B**34**, 3444–3446.

Wiesbrock, F. & Schmidbaur, H. (2003). *J. Am. Chem. Soc.* **125**, 3622–3630.

Wiesbrock, F. & Schmidbaur, H. (2004). *J. Inorg. Biochem.* **98**, 473–484.

supporting information

Acta Cryst. (2020). E**76**, 328-331 [https://doi.org/10.1107/S2056989020001577]

Crystal structure of poly[(μ_3-4-amino-1,2,5-oxadiazole-3-hydroxamato)thallium(I)]

Inna S. Safyanova, Oksana A. Bondar, Anna V. Pavlishchuk, Iryna V. Omelchenko, Turganbay S. Iskenderov and Valentina A. Kalibabchuk

Computing details

Data collection: *CrysAlis PRO* (Agilent, 2012); cell refinement: *CrysAlis PRO* (Agilent, 2012); data reduction: *CrysAlis PRO* (Agilent, 2012); program(s) used to solve structure: SHELXT (Sheldrick, 2015); program(s) used to refine structure: *olex2.refine* (Bourhis *et al.*, 2015); molecular graphics: *OLEX2* (Dolomanov *et al.*, 2009); software used to prepare material for publication: *OLEX2* (Dolomanov *et al.*, 2009).

Poly[(μ_3-4-amino-1,2,5-oxadiazole-3-hydroxamato)thallium(I)]

Crystal data

$[Tl(C_3H_3N_4O_3)]$
M_r = 347.46
Monoclinic, $P2_1/c$
a = 10.0731 (4) Å
b = 3.74576 (18) Å
c = 16.9805 (6) Å
β = 95.808 (4)°
V = 637.41 (5) Å^3
Z = 4
$F(000)$ = 612
D_x = 3.610 Mg m^{-3}
Mo $K\alpha$ radiation, λ = 0.71073 Å
Cell parameters from 216 reflections
θ = 4.4–22.3°
μ = 25.30 mm^{-1}
T = 298 K
Block, clear colourless
0.2 × 0.2 × 0.2 mm

Data collection

Agilent Xcalibur Sapphire3 CCD diffractometer
ω scans
Absorption correction: multi-scan (*CrysAlis PRO*; Agilent, 2012)
T_{min} = 0.231, T_{max} = 1.000
4634 measured reflections
1452 independent reflections
1320 reflections with $I > 2\sigma(I)$
R_{int} = 0.056
θ_{max} = 27.5°, θ_{min} = 3.0°
h = −13→13
k = −4→4
l = −22→19

Refinement

Refinement on F^2
Least-squares matrix: full
$R[F^2 > 2\sigma(F^2)]$ = 0.045
$wR(F^2)$ = 0.111
S = 1.07
1452 reflections
100 parameters
0 restraints
Hydrogen site location: difference Fourier map
H-atom parameters constrained
$w = 1/[\sigma^2(F_o^2) + (0.0629P)^2]$ where $P = (F_o^2 + 2F_c^2)/3$
$(\Delta/\sigma)_{max}$ = 0.001
$\Delta\rho_{max}$ = 6.17 e Å^{-3}
$\Delta\rho_{min}$ = −2.23 e Å^{-3}

Special details

Geometry. All esds (except the esd in the dihedral angle between two l.s. planes) are estimated using the full covariance matrix. The cell esds are taken into account individually in the estimation of esds in distances, angles and torsion angles; correlations between esds in cell parameters are only used when they are defined by crystal symmetry. An approximate (isotropic) treatment of cell esds is used for estimating esds involving l.s. planes.

Fractional atomic coordinates and isotropic or equivalent isotropic displacement parameters (Å²)

	x	*y*	*z*	U_{iso}*/U_{eq}
Tl1	0.05880 (4)	0.45183 (11)	0.86058 (2)	0.03141 (19)
O2	0.1164 (7)	0.4279 (17)	0.7187 (4)	0.0298 (15)
O1	0.2851 (8)	0.0779 (19)	0.8210 (4)	0.0339 (17)
O3	0.2375 (8)	0.4924 (18)	0.4946 (5)	0.0339 (17)
N2	0.1809 (10)	0.510 (2)	0.5642 (6)	0.0299 (19)
N1	0.3245 (8)	0.148 (2)	0.7450 (4)	0.0301 (17)
C1	0.2298 (9)	0.319 (2)	0.7013 (5)	0.0257 (18)
N4	0.4966 (9)	0.110 (2)	0.6207 (5)	0.0339 (19)
H4A	0.528766	−0.041040	0.583376	0.041*
H4B	0.482666	0.024160	0.675476	0.041*
N3	0.3648 (8)	0.328 (2)	0.5070 (4)	0.0332 (18)
C2	0.2653 (9)	0.367 (3)	0.6185 (5)	0.0267 (18)
C3	0.3828 (9)	0.254 (2)	0.5839 (5)	0.0243 (17)

Atomic displacement parameters (Å²)

	U^{11}	U^{22}	U^{33}	U^{12}	U^{13}	U^{23}
Tl1	0.0281 (3)	0.0419 (3)	0.0240 (3)	0.00530 (14)	0.00185 (18)	−0.00084 (13)
O2	0.019 (3)	0.047 (4)	0.024 (3)	0.002 (3)	0.004 (3)	−0.002 (3)
O1	0.026 (4)	0.053 (4)	0.023 (4)	0.001 (3)	0.004 (3)	0.006 (3)
O3	0.030 (4)	0.049 (4)	0.023 (4)	0.001 (3)	0.002 (3)	0.003 (3)
N2	0.028 (5)	0.040 (4)	0.022 (4)	0.004 (3)	0.003 (4)	0.003 (3)
N1	0.027 (4)	0.041 (4)	0.023 (4)	0.005 (4)	0.005 (3)	0.002 (3)
C1	0.032 (5)	0.024 (4)	0.022 (4)	−0.002 (4)	0.003 (4)	−0.004 (3)
N4	0.031 (5)	0.044 (5)	0.029 (4)	0.008 (4)	0.011 (4)	−0.001 (4)
N3	0.028 (4)	0.042 (5)	0.028 (4)	0.009 (4)	0.000 (3)	0.002 (4)
C2	0.020 (4)	0.029 (4)	0.030 (5)	−0.002 (4)	−0.001 (4)	−0.005 (4)
C3	0.023 (4)	0.030 (4)	0.020 (4)	−0.004 (3)	0.000 (3)	−0.006 (3)

Geometric parameters (Å, º)

Tl1—O2	2.537 (7)	O1—N1	1.412 (9)
Tl1—O2^{i}	2.761 (7)	O3—N2	1.365 (11)
Tl1—O1	2.814 (7)	O3—N3	1.419 (11)
Tl1—O2^{ii}	2.880 (7)	N2—C2	1.304 (14)
Tl1—O3^{iii}	3.219 (8)	N1—C1	1.314 (12)
Tl1—N2^{ii}	3.289 (9)	C1—C2	1.497 (11)
Tl1—C1^{i}	3.291 (9)	N4—C3	1.360 (13)
Tl1—O1^{iv}	3.385 (7)	N4—H4A	0.9324

Tl1—C1	3.387 (8)	N4—H4B	1.0077
Tl1—O3^{v}	3.453 (8)	N3—C3	1.329 (11)
O2—C1	1.275 (11)	C2—C3	1.437 (11)

O2—Tl1—O2^{i}	75.9 (2)	N1—O1—Tl1^{vi}	124.6 (6)
O2—Tl1—O1	59.1 (2)	Tl1—O1—Tl1^{vi}	73.70 (15)
O2^{i}—Tl1—O1	134.3 (2)	N1—O1—Tl1^{ii}	69.9 (5)
O2—Tl1—O2^{ii}	73.8 (2)	Tl1—O1—Tl1^{ii}	67.89 (16)
O2^{i}—Tl1—O2^{ii}	83.2 (2)	Tl1^{vi}—O1—Tl1^{ii}	64.47 (13)
O1—Tl1—O2^{ii}	91.3 (2)	N2—O3—N3	110.1 (8)
O2—Tl1—O3^{iii}	119.2 (2)	N2—O3—Tl1^{vii}	112.7 (6)
O2^{i}—Tl1—O3^{iii}	164.3 (2)	N3—O3—Tl1^{vii}	108.2 (5)
O1—Tl1—O3^{iii}	60.21 (19)	N2—O3—Tl1^{viii}	107.8 (5)
O2^{ii}—Tl1—O3^{iii}	104.50 (19)	N3—O3—Tl1^{viii}	139.7 (5)
O2—Tl1—O1^{iv}	67.2 (2)	Tl1^{vii}—O3—Tl1^{viii}	68.20 (17)
O2^{i}—Tl1—O1^{iv}	82.28 (19)	N2—O3—Tl1^{i}	29.7 (5)
O1—Tl1—O1^{iv}	73.70 (16)	N3—O3—Tl1^{i}	137.7 (5)
O2^{ii}—Tl1—O1^{iv}	140.56 (18)	Tl1^{vii}—O3—Tl1^{i}	103.6 (2)
O3^{iii}—Tl1—O1^{iv}	99.15 (19)	Tl1^{viii}—O3—Tl1^{i}	78.16 (14)
O2—Tl1—O3^{v}	119.6 (2)	N2—O3—Tl1^{ii}	36.6 (5)
O2^{i}—Tl1—O3^{v}	101.3 (2)	N3—O3—Tl1^{ii}	111.1 (5)
O1—Tl1—O3^{v}	94.4 (2)	Tl1^{vii}—O3—Tl1^{ii}	78.51 (15)
O2^{ii}—Tl1—O3^{v}	166.55 (18)	Tl1^{viii}—O3—Tl1^{ii}	107.4 (2)
O3^{iii}—Tl1—O3^{v}	68.20 (17)	Tl1^{i}—O3—Tl1^{ii}	49.53 (8)
O1^{iv}—Tl1—O3^{v}	52.89 (17)	C2—N2—O3	107.0 (8)
Tl1—O2—Tl1^{ii}	106.8 (2)	C1—N1—O1	110.6 (7)
C1—O2—Tl1^{i}	129.1 (6)	O2—C1—N1	129.9 (8)
Tl1—O2—Tl1^{i}	103.4 (2)	O2—C1—C2	118.9 (9)
Tl1^{ii}—O2—Tl1^{i}	83.2 (2)	N1—C1—C2	111.1 (7)
C1—O2—Tl1^{vi}	91.8 (5)	C3—N4—H4A	105.2
Tl1—O2—Tl1^{vi}	57.29 (13)	C3—N4—H4B	111.1
Tl1^{ii}—O2—Tl1^{vi}	67.75 (13)	H4A—N4—H4B	121.6
Tl1^{i}—O2—Tl1^{vi}	134.9 (2)	C3—N3—O3	105.6 (6)
C1—O2—Tl1^{iv}	123.5 (6)	N2—C2—C3	109.7 (8)
Tl1—O2—Tl1^{iv}	54.51 (12)	N2—C2—C1	120.8 (8)
Tl1^{ii}—O2—Tl1^{iv}	133.3 (2)	C3—C2—C1	129.3 (9)
Tl1^{i}—O2—Tl1^{iv}	64.69 (12)	N3—C3—N4	124.0 (7)
Tl1^{vi}—O2—Tl1^{iv}	111.80 (14)	N3—C3—C2	107.6 (8)
N1—O1—Tl1	115.8 (5)	N4—C3—C2	128.3 (8)

N3—O3—N2—C2	−0.1 (10)	Tl1^{vi}—N1—C1—Tl1^{i}	74.4 (19)
Tl1^{vii}—O3—N2—C2	120.8 (7)	O1—N1—C1—Tl1^{vi}	−38.2 (6)
Tl1^{viii}—O3—N2—C2	−166.0 (6)	Tl1—N1—C1—Tl1^{vi}	−48.4 (2)
Tl1^{i}—O3—N2—C2	−161.9 (14)	Tl1^{ii}—N1—C1—Tl1^{vi}	29.4 (5)
Tl1^{ii}—O3—N2—C2	98.6 (9)	N2—O3—N3—C3	−0.6 (10)
N3—O3—N2—Tl1^{i}	161.8 (7)	Tl1^{vii}—O3—N3—C3	−124.1 (6)
Tl1^{vii}—O3—N2—Tl1^{i}	−77.3 (8)	Tl1^{viii}—O3—N3—C3	158.3 (6)
Tl1^{viii}—O3—N2—Tl1^{i}	−4.1 (10)	Tl1^{i}—O3—N3—C3	12.7 (11)

Tl1^{ii}—O3—N2—Tl1^{i}	−99.5 (12)	Tl1^{ii}—O3—N3—C3	−39.7 (8)
N3—O3—N2—Tl1^{ii}	−98.7 (9)	N2—O3—N3—Tl1^{vii}	123.5 (7)
Tl1^{vii}—O3—N2—Tl1^{ii}	22.2 (9)	Tl1^{viii}—O3—N3—Tl1^{vii}	−77.5 (7)
Tl1^{viii}—O3—N2—Tl1^{ii}	95.4 (6)	Tl1^{i}—O3—N3—Tl1^{vii}	136.8 (8)
Tl1^{i}—O3—N2—Tl1^{ii}	99.5 (12)	Tl1^{ii}—O3—N3—Tl1^{vii}	84.4 (3)
N3—O3—N2—Tl1^{vii}	−120.9 (7)	N2—O3—N3—Tl1^{viii}	−158.9 (12)
Tl1^{viii}—O3—N2—Tl1^{vii}	73.2 (4)	Tl1^{vii}—O3—N3—Tl1^{viii}	77.5 (7)
Tl1^{i}—O3—N2—Tl1^{vii}	77.3 (8)	Tl1^{i}—O3—N3—Tl1^{viii}	−145.6 (13)
Tl1^{ii}—O3—N2—Tl1^{vii}	−22.2 (9)	Tl1^{ii}—O3—N3—Tl1^{viii}	161.9 (10)
N3—O3—N2—Tl1^{viii}	165.9 (8)	O3—N2—C2—C3	0.7 (11)
Tl1^{vii}—O3—N2—Tl1^{viii}	−73.2 (4)	Tl1^{i}—N2—C2—C3	−166.4 (6)
Tl1^{i}—O3—N2—Tl1^{viii}	4.1 (10)	Tl1^{ii}—N2—C2—C3	131.4 (7)
Tl1^{ii}—O3—N2—Tl1^{viii}	−95.4 (6)	Tl1^{vii}—N2—C2—C3	52.0 (10)
Tl1—O1—N1—C1	−13.7 (9)	Tl1^{viii}—N2—C2—C3	−29 (2)
Tl1^{vi}—O1—N1—C1	73.8 (9)	O3—N2—C2—C1	−175.4 (8)
Tl1^{ii}—O1—N1—C1	37.9 (6)	Tl1^{i}—N2—C2—C1	17.5 (11)
Tl1^{vi}—O1—N1—Tl1	87.4 (6)	Tl1^{ii}—N2—C2—C1	−44.7 (8)
Tl1^{ii}—O1—N1—Tl1	51.6 (4)	Tl1^{vii}—N2—C2—C1	−124.2 (7)
Tl1—O1—N1—Tl1^{ii}	−51.6 (4)	Tl1^{viii}—N2—C2—C1	154.6 (11)
Tl1^{vi}—O1—N1—Tl1^{ii}	35.9 (5)	O3—N2—C2—Tl1^{ii}	−130.7 (7)
Tl1—O1—N1—Tl1^{vi}	−87.4 (6)	Tl1^{i}—N2—C2—Tl1^{ii}	62.2 (4)
Tl1^{ii}—O1—N1—Tl1^{vi}	−35.9 (5)	Tl1^{vii}—N2—C2—Tl1^{ii}	−79.4 (5)
Tl1—O2—C1—N1	13.2 (13)	Tl1^{viii}—N2—C2—Tl1^{ii}	−160.6 (16)
Tl1^{ii}—O2—C1—N1	−106.2 (10)	O3—N2—C2—Tl1^{i}	167.1 (9)
Tl1^{i}—O2—C1—N1	162.0 (7)	Tl1^{ii}—N2—C2—Tl1^{i}	−62.2 (4)
Tl1^{vi}—O2—C1—N1	−38.7 (10)	Tl1^{vii}—N2—C2—Tl1^{i}	−141.7 (8)
Tl1^{iv}—O2—C1—N1	79.1 (11)	Tl1^{viii}—N2—C2—Tl1^{i}	137.1 (18)
Tl1—O2—C1—C2	−170.2 (6)	O2—C1—C2—N2	−1.5 (14)
Tl1^{ii}—O2—C1—C2	70.4 (8)	N1—C1—C2—N2	175.7 (9)
Tl1^{i}—O2—C1—C2	−21.4 (12)	Tl1^{ii}—C1—C2—N2	48.9 (9)
Tl1^{vi}—O2—C1—C2	137.9 (7)	Tl1—C1—C2—N2	−18 (2)
Tl1^{iv}—O2—C1—C2	−104.3 (8)	Tl1^{i}—C1—C2—N2	−13.9 (9)
Tl1—O2—C1—Tl1^{ii}	119.5 (6)	Tl1^{vi}—C1—C2—N2	95.3 (11)
Tl1^{i}—O2—C1—Tl1^{ii}	−91.7 (7)	O2—C1—C2—C3	−176.8 (9)
Tl1^{vi}—O2—C1—Tl1^{ii}	67.6 (2)	N1—C1—C2—C3	0.4 (14)
Tl1^{iv}—O2—C1—Tl1^{ii}	−174.7 (6)	Tl1^{ii}—C1—C2—C3	−126.4 (9)
Tl1^{ii}—O2—C1—Tl1	−119.5 (6)	Tl1—C1—C2—C3	166.8 (11)
Tl1^{i}—O2—C1—Tl1	148.8 (10)	Tl1^{i}—C1—C2—C3	170.8 (10)
Tl1^{vi}—O2—C1—Tl1	−51.9 (4)	Tl1^{vi}—C1—C2—C3	−80.0 (13)
Tl1^{iv}—O2—C1—Tl1	65.8 (5)	O2—C1—C2—Tl1^{ii}	−50.4 (7)
Tl1—O2—C1—Tl1^{i}	−148.8 (10)	N1—C1—C2—Tl1^{ii}	126.8 (8)
Tl1^{ii}—O2—C1—Tl1^{i}	91.7 (7)	Tl1—C1—C2—Tl1^{ii}	−66.7 (14)
Tl1^{vi}—O2—C1—Tl1^{i}	159.3 (7)	Tl1^{i}—C1—C2—Tl1^{ii}	−62.78 (17)
Tl1^{iv}—O2—C1—Tl1^{i}	−82.9 (6)	Tl1^{vi}—C1—C2—Tl1^{ii}	46.4 (7)
Tl1—O2—C1—Tl1^{vi}	51.9 (4)	O2—C1—C2—Tl1^{i}	12.4 (7)
Tl1^{ii}—O2—C1—Tl1^{vi}	−67.6 (2)	N1—C1—C2—Tl1^{i}	−170.4 (8)
Tl1^{i}—O2—C1—Tl1^{vi}	−159.3 (7)	Tl1^{ii}—C1—C2—Tl1^{i}	62.78 (17)
Tl1^{iv}—O2—C1—Tl1^{vi}	117.8 (5)	Tl1—C1—C2—Tl1^{i}	−3.9 (14)

O1—N1—C1—O2	1.8 (14)	Tl1^{vi}—C1—C2—Tl1^{i}	109.2 (8)
Tl1—N1—C1—O2	−8.4 (9)	O3—N3—C3—N4	−176.4 (8)
Tl1^{ii}—N1—C1—O2	69.4 (9)	Tl1^{vii}—N3—C3—N4	130.2 (8)
Tl1^{vi}—N1—C1—O2	40.0 (11)	Tl1^{viii}—N3—C3—N4	−162.5 (7)
O1—N1—C1—C2	−175.0 (8)	O3—N3—C3—C2	1.0 (10)
Tl1—N1—C1—C2	174.8 (8)	Tl1^{vii}—N3—C3—C2	−52.4 (10)
Tl1^{ii}—N1—C1—C2	−107.4 (9)	Tl1^{viii}—N3—C3—C2	14.8 (11)
Tl1^{vi}—N1—C1—C2	−136.8 (6)	Tl1^{ix}—N4—C3—N3	29.1 (18)
O1—N1—C1—Tl1^{ii}	−67.6 (9)	Tl1^{ix}—N4—C3—C2	−147.8 (9)
Tl1—N1—C1—Tl1^{ii}	−77.8 (4)	N2—C2—C3—N3	−1.1 (11)
Tl1^{vi}—N1—C1—Tl1^{ii}	−29.4 (5)	C1—C2—C3—N3	174.6 (9)
O1—N1—C1—Tl1	10.2 (7)	Tl1^{ii}—C2—C3—N3	85.0 (10)
Tl1^{ii}—N1—C1—Tl1	77.8 (4)	Tl1^{i}—C2—C3—N3	−27.9 (19)
Tl1^{vi}—N1—C1—Tl1	48.4 (2)	N2—C2—C3—N4	176.1 (9)
O1—N1—C1—Tl1^{i}	36 (2)	C1—C2—C3—N4	−8.2 (16)
Tl1—N1—C1—Tl1^{i}	26.0 (17)	Tl1^{ii}—C2—C3—N4	−97.8 (11)
Tl1^{ii}—N1—C1—Tl1^{i}	103.8 (19)	Tl1^{i}—C2—C3—N4	149.3 (12)

Symmetry codes: (i) −*x*, *y*+1/2, −*z*+3/2; (ii) −*x*, *y*−1/2, −*z*+3/2; (iii) *x*, −*y*+1/2, *z*+1/2; (iv) *x*, *y*+1, *z*; (v) *x*, −*y*+3/2, *z*+1/2; (vi) *x*, *y*−1, *z*; (vii) *x*, −*y*+1/2, *z*−1/2; (viii) *x*, −*y*+3/2, *z*−1/2; (ix) −*x*+1, *y*−1/2, −*z*+3/2.

Hydrogen-bond geometry (Å, º)

D—H···*A*	*D*—H	H···*A*	*D*···*A*	*D*—H···*A*
N4—H4*A*···N3^{x}	0.93	2.23	3.156 (10)	169
N4—H4*B*···N1^{ix}	1.01	2.65	3.256 (13)	118

Symmetry codes: (ix) −*x*+1, *y*−1/2, −*z*+3/2; (x) −*x*+1, −*y*, −*z*+1.